Bull. Nov. Comp. Center, Num. Model. in Atmosph., etc., 2 (1995), 13–30

North Pasific diagnostic circulation model*

V.I. Kuzin and V.M. Moiseev

Numerical diagnostic model, based on the finite element method [1] is presented in the paper. Numerical experiments for the estimation of the role of wind and thermohaline factors in the North Pacific basin were carried out by the model. Diagnostic calculations both the integral stream function and 3-d baroclinic velocity fields were done with the use of the wind-stress [2], temperature and salinity data [3]. The one-two degree resolution was used for the basin, with the tropical zone included until 30,5° S.

Numerical results and the comparison with the results of the papers [4, 5] are presented.

1. Ocean circulation diagnostic model

System of equations for diagnostic calculations of the 3-d velocity fields by the temperature and salinity fields prescribed has the form:

$$\frac{\partial U}{\partial t} + (f - \delta)\vec{k} \cdot U = -\frac{1}{\rho_0}\nabla P + \frac{\partial}{\partial z} v \frac{\partial U}{\partial z} + \vec{F}, \tag{1}$$

$$\operatorname{div} U + \frac{\partial w}{\partial z} = 0, \tag{2}$$

$$\frac{\partial P}{\partial z} = g\rho, \tag{3}$$

$$\rho = \rho(T, S). \tag{4}$$

The equations (1)–(4) are written in coordinates (λ, θ, z) on the sphere of the radius a; λ – longitude, $\theta = \varphi + \pi/2$, φ – latitude, z – vertical coordinate with the positive direction from the surface to the center of the Earth. $U = (u, v)$ – vector of horizontal velocity components, w – vertical velocity component, $m = 1/a \sin\theta$, $n = 1/a$, $a = 6.38 \times 10^8$cm, $f = 2\omega\cos\theta$ – Coriolis parameter, $\omega = 0.73 \times 10^{-4}$ – angular speed of the Earth rotation, $\rho_0 = \text{const}$ – standard density, ρ – density, P – pressure, ν – vertical mixing coefficient, T – temperature (°C), S – salinity (‰), $\vec{k}$ – unit vector by z-direction, $\delta = m\cos\theta u$,

*Supported by the Russian Fund of Fundamental Research under Grant 93-05-08993.

$$\nabla P = \left(m\frac{\partial P}{\partial \lambda}, n\frac{\partial P}{\partial \theta}\right), \qquad \operatorname{div} U = m\left(\frac{\partial u}{\partial \lambda} + \frac{\partial}{\partial \theta}\frac{n}{m}v\right),$$

$$F = A_l\Big(m\Delta U + (n^2 - m^2\cos^2\theta)U - 2m^2\cos\theta\cdot\vec{k}\times\frac{\partial U}{\partial \lambda}\Big),$$

where A_l is the horizontal mixing coefficient,

$$\Delta\varphi = \frac{\partial}{\partial \lambda}m\frac{\partial \varphi}{\partial \lambda} + \frac{\partial}{\partial \theta}\frac{n^2}{m}\frac{\partial \varphi}{\partial \theta},$$

$$\frac{\partial \varphi}{\partial t} = \frac{\partial \varphi}{\partial t} + mu\frac{\partial \varphi}{\partial \lambda} + nv\frac{\partial \varphi}{\partial \theta} + w\frac{\partial \varphi}{\partial z}.$$

Boundary conditions for (1)–(4) are as follows:

at the surface ($z = 0$): $w = 0, \quad \nu\dfrac{\partial U}{\partial z} = -\dfrac{\vec{\tau}}{\rho},$ (5)

at the bottom ($z = H(\lambda, \theta)$):

$$w = U\cdot\nabla H, \quad \nu\frac{\partial U}{\partial z} = -R\overline{U}, \quad \Big(\overline{U} = \frac{1}{H}\int_0^H U dz\Big),$$ (6)

at the cylindrical lateral boundaries ($\Gamma = \Gamma_0 \cup \Gamma_1$):

a) 'solid' boundary (Γ_0): $\dfrac{\partial U\vec{l}}{\partial n} = 0, \quad U\vec{n} = 0,$ (7)

b) 'liquid' boundary (Γ_1): $U = U^0.$ (8)

In the relations (5)–(8) $\vec{\tau}$ – wind-stress vector, R – bottom drag coefficient, $\vec{l}$, $\vec{n}$ – tangent and normal unit vectors of the lateral and normal directions to the boundary Γ accordingly. Index (°) marks the values, which are specified. At the initial time values u^0 and v^0 are prescribed. Solution of the system of equations (1)–(8) is carried out by traditional technique [6] by separating of the external (barotropic) and internal (baroclinic) modes. For this purpose velocity field U is presented as a sum $U = \overline{U} + U'$, where $\overline{U} = \frac{1}{H}\int_0^H U dz$, $U' = U - \overline{U}$.

For the determination of the external mode component $\overline{U}$ the integral stream function ψ is used. The equation for this function is derived from (1) averaged by the vertical by applying the operation rot_z. As a result the integral vorticity equation in the term of the integral stream function can be presented in the form:

$$\frac{\partial}{\partial t}\Big(\nabla\Big(\frac{1}{H}\nabla\psi\Big)\Big) + \nabla\Big(\frac{R}{H}\nabla\psi\Big) - \operatorname{rot}_z(\xi^*\nabla\psi) = -\operatorname{rot}_z\Big(-\frac{1}{\rho_0 H}\int_0^H \nabla p dz\Big) -$$

$$\operatorname{rot}_z\frac{1}{H}\int_0^H L(U')dz + \operatorname{rot}_z\frac{\tau}{\rho_0 H} + A_l\nabla(\nabla H\xi), \quad H\xi = \nabla\Big(\frac{1}{H}\nabla\psi\Big),$$ (9)

where $\xi^* = \xi + \frac{f}{H}$, $\mathrm{rot}_z \vec{q} = m\left(\frac{\partial q_2}{\partial \lambda} - \frac{\partial}{\partial \theta}\frac{n}{m}q_1\right)$, $\vec{q} = (q_1, q_2)$, with the boundary conditions:

$$\begin{aligned} &\text{at } \Gamma_0: \quad \psi = 0, \ \xi = 0, \\ &\text{at } \Gamma_1: \quad \psi = \psi^0, \ \xi = \xi^0. \end{aligned} \tag{10}$$

Equations for U' have the form:

$$\frac{\partial U'}{\partial t} + L(U') = -\frac{1}{\rho_0}\left(\nabla P - \frac{1}{H}\int_0^H \nabla P dz\right) + \frac{\partial}{\partial z}\nu\frac{\partial U'}{\partial z} - \frac{1}{H}\left(\nu\frac{\partial U'}{\partial z}\right)_0^H + \frac{1}{H}\int_0^H L(U')dz - I. \tag{11}$$

Here

$$L(U') = mu\frac{\partial U'}{\partial \lambda} + nu\frac{\partial U'}{\partial \theta} + w\frac{\partial U'}{\partial z} + (f - \delta)\cdot\vec{k}\times U' - A_l\left[m\Delta U' + (n^2 - m^2\cos^2\theta)U' - 2m^2\cos\theta\vec{k}\times\frac{\partial U'}{\partial \lambda}\right],$$

$$I = mu'\frac{\partial \vec{U}}{\partial \lambda} + nv'\frac{\partial \vec{U}}{\partial \theta} + m\vec{U}u'\cos\theta.$$

Advective terms in (11) are transformed before discretization from gradient to special divergent form with the using of some potential function analogues

$$\hat{u} = -\int_0^z u dz, \quad \hat{v} = -\int_0^z v dz.$$

Vertical velocity component can be determined from the relation

$$w = m\left(\frac{\partial \hat{u}}{\partial \lambda} + \frac{\partial}{\partial \theta}\frac{n}{m}\hat{v}\right).$$

With the using of these relations advective terms can be written as follows:

$$BU' \equiv mu\frac{\partial U'}{\partial \lambda} + nv\frac{\partial U'}{\partial \theta} + w\frac{\partial U'}{\partial z} = m\left(\frac{\partial}{\partial \lambda}\hat{u}\frac{\partial U'}{\partial z} - \frac{\partial}{\partial z}\hat{u}\frac{\partial U}{\partial \lambda}\right) + m\left(\frac{\partial}{\partial \theta}\frac{n}{m}\hat{v}\frac{\partial U'}{\partial z} - \frac{\partial}{\partial z}\frac{n}{m}\hat{v}\frac{\partial U'}{\partial \theta}\right).$$

2. Additional notations

Let us denote the 3-D domain of the basin by D, with the lateral boundary Γ. Then we denote the inner product for the scalar functions φ, ψ

$$(\varphi, \rho) = \int_\Omega \varphi\rho \, d\Omega, \quad d\Omega = \frac{d\lambda d\theta}{mn}.$$

For vector functions F and Q ($F = (F_\lambda, F_\theta)$, $Q = (Q_\lambda, Q_\theta)$) the inner product will have the form

$$\text{at the domain } \Omega: \quad (F, Q)_\Omega = \int_\Omega (F_\lambda Q_\lambda + F_\theta Q_\theta)\, d\Omega \equiv \int_\Omega F \cdot Q \, d\Omega,$$

$$\text{at } D = \Omega \times [0, H]: \quad (U, V) = \int_D uv \, dD, \quad dD = dz \, d\Omega.$$

Now we describe the discrete analogues of D and Ω which we denote D^h and Ω^h corresponingly. For the boundaries Γ and S the notations Γ^h and S^h are used.

Triangulation of the 2-D domain is carried out as follows: the uniform grid with the steps $\Delta\lambda = h_\lambda = 2°$, $\Delta\theta = h_\theta = 1°$ is introduced. After this the triangulation of the domain is made by the diagonals of the rectangular cells of positive and negative direction in turn. The distribution of the triangles vertices forms the "chess" grid. These nodes are associated with the fields T, S, P, Ψ. The grid we will call the "main". For denoting the velocity components u, v the nodes are shifted relatively the main grid on the half of the step. This combination is the triangulated analog of the E-grid by the Arakawa classification [7]. By the vertical direction 18 levels are introduced: T, S, P, u, v - are associated with the integer index levels, while w - with the half-integer index levels. One can represent the domain as a combination of the triangles. Summing all of the triangles with the common vertex R gives the support (Figure 1). Figure 2 represents the nodal distributions for the different values by the vertical $3D$ cells is the combination of the prisms with the support (Figure 1) and the height $\Delta Z_n = Z_{n+\frac{1}{2}} - Z_{n-\frac{1}{2}} = (Z_{n+1} - Z_{n-1})/2$, where n is the number of the level $n = 1, N$.

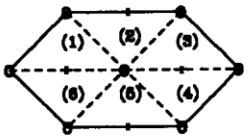

Figure 1. Main support: o – scalar points; x – vector points

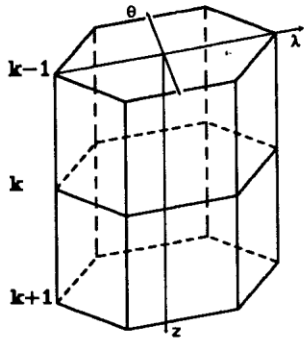

Figure 2. 3-D cell

In addition, the barycentric ($B-$) cells in the Ω_R^h are also used for the "mass lumping" representation for some terms.

3. FEM discretization of the integral stream function equation

For the use of the Galerkin procedure for (9) discretization the weak form of the problem is needed. For this purpose let us consider the integral relations for $\Psi, \xi \in W_2^1(\Omega)$

$$-\frac{\partial}{\partial t}\left(\frac{1}{H}\nabla\Psi, \nabla\Phi\right)_\Omega - \left(\frac{R}{H^2}\nabla\Psi, \nabla\Phi\right)_\Omega - (\mathrm{rot}_z(\xi^*\nabla\Psi), \Phi)_\Omega =$$

$$-\mathrm{rot}_z\left(\frac{1}{\rho_0 H}\int_0^H \nabla P dz, \Phi\right)_\Omega + \left(\mathrm{rot}_z\frac{\tau}{\rho H}, \Phi\right)_\Omega, \qquad (12)$$

$$(H\xi, \Phi)_\Omega = \left(\frac{1}{H}\nabla\Psi, \nabla\Phi\right)_\Omega, \qquad \forall\Phi \in W_2^1(\Omega). \qquad (13)$$

Here $\xi^* = \xi/H + f$. In the relation the influence of the vertically averaged nonlinear term as well as horizontal mixing term were neglected. The coordinate function Φ for nodal point R is the piece-wise linear one, defined at the support Ω_R. It is equal to one at the node R and has the support 0 in any nodes of Ω^h. $\Phi(\lambda, \theta)$ can be presented in the form

$$\Phi_R^{(i)}(\lambda, \theta) = 1 + \alpha_R^{(i)}\frac{\lambda - \lambda_R}{h_\lambda} + \beta_R^{(i)}\frac{\theta - \theta_R}{h_\theta},$$

where (i) is the number of the triangles included to the support

$$\alpha_R^{(i)} = \frac{\partial\Phi_R^{(i)}}{\partial\lambda}h_\lambda, \quad \beta_R^{(i)} = \frac{\partial\Phi_R}{\partial\theta}h_\theta.$$

Using these notations the function is presented as the linear combination

$$\Psi = \sum_{i=1}^{\tau}\sum_{\Delta i}\Psi_{q(i)}\Phi_{q(i)}^{(i)}(\lambda, \theta).$$

Here Δ_i is the i-th triangle of Ω_R and $q(i)$ is its vortices. Let us write out the representation of the terms of equation (12) for the R node:

1. The first two terms have the form

$$\left(\frac{1}{H}\nabla\Psi, \nabla\Phi_R\right)_{\Omega_R^h} = \int_{\Omega_R^h}\frac{1}{H}\left(m^2\frac{\partial\Psi}{\partial\lambda}\frac{\partial\Phi_R}{\partial\lambda} + n^2\frac{\partial\Psi}{\partial\theta}\frac{\partial\Phi_R}{\partial\theta}\right)d\Omega =$$

$$\frac{h_\lambda}{2h_\theta}\left(A^{(1)} + A^{(6)}\right)\Psi_A + \left(B^{(1)} + B^{(2)}\right)\Psi_B + \left(C^{(2)} + C^{(3)}\right)\Psi_C +$$

$$\left(D^{(3)} + D^{(4)}\right)\Psi_D + \left(E^{(4)} + E^{(5)}\right)\Psi_E + \left(F^{(5)} + F^{(6)}\right)\Psi_F + R^{(0)}\Psi_R,$$

$$R^{(0)} = \sum_i R^{(i)}, \quad i = \overline{1,6}. \qquad (14)$$

Let us consider, for example, the integral by the first triangle (Figure 1). Here

$$
\begin{aligned}
A^{(1)} &= \left(\overline{\frac{1}{H}}\right)\left[(\overline{m})^{(1)}\left(\frac{h_0}{h_\lambda}\right)^2\alpha_R^{(1)}\alpha_A^{(1)} + (\overline{n^2/m})^{(1)}\beta_R^{(1)}\beta_A^{(1)}\right], \\
B^{(1)} &= \left(\overline{\frac{1}{H}}\right)^{(1)}\left[\overline{m}^{(1)}\left(\frac{h_0}{h_\lambda}\right)^2\alpha_R^{(1)}\alpha_B^{(1)} + (\overline{n^2/m})^{(2)}\beta_R^{(1)}\beta_B^{(1)}\right], \qquad (15) \\
R^{(1)} &= -(A^{(1)} + B^{(1)}),
\end{aligned}
$$

where bar marks the averaging by the triangle i.e., $\overline{\varphi} = \frac{1}{S_\Delta}\int_\Delta \varphi ds$. A, B, R – vertices of the triangle Δ_1; $A^{(1)}$, $B^{(1)}$, $R^{(1)}$ are the coefficients values in the vortices.

The coefficients for another triangles can be obtained in the same way. The relation (15) is produced by the summation of the integrals for all triangles.

The discrete form for the bottom drag term has the same form. In this case the coefficient $1/H$ in (15) has to be changed by R/H.

2. Advective terms are combined with the planetary vorticity term. Let us consider the relation

$$
-\operatorname{rot}_z(\varphi\nabla\Psi) = -J(\varphi,\Psi) = \tau(\Psi,\varphi),
$$

where

$$
J(\Psi,\varphi) = mn\left(\frac{\partial\Psi}{\partial\lambda}\frac{\partial\varphi}{\partial\theta} - \frac{\partial\Psi}{\partial\theta}\frac{\partial\varphi}{\partial\lambda}\right).
$$

The associated integral relations have the form

$$
(-\operatorname{rot}_z(\varphi\nabla\Psi), \Phi_R)_{\Omega_R^h} = (-J(\varphi,\Psi), \Phi_R)_{\Omega_R^h}.
$$

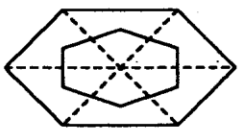

Figure 3. Barycentric (B–) cell

The discretization for the latter formula was carried out with the use of the lumping procedure on the baricentric (B)-cell (Figure 3). This permits to construct the up-stream mass-conserving scheme for the term [1]. Without presentation the details of this procedure here, let us write out the final discrete operator, which can be presented as follows:

$$
\left(J(\varphi,\Psi), \hat{\Phi}_r\right)_{\hat{\Omega}_R^h} = A_j\Psi_A + B_j\Psi_B + C_j\Psi_C + D_jC_D + E_j\Psi_E + F_j\Psi_E + R_j\Psi_R.
$$

$$A_j = \frac{A^* - |A^*|}{2}, \quad B_j = \frac{B^* - |B^*|}{2}, \quad C_j = \frac{C^* - |C^*|}{2},$$
$$D_j = \frac{D^* - |D^*|}{2}, \quad E_j = \frac{E^* - |E^*|}{2}, \quad F_j = \frac{F^* - |F^*|}{2},$$
$$R_j = (A_j + B_j + C_j + Dj + E_j + F_j),$$
$$A^* = \overline{\varphi}^{(1)} - \overline{\varphi}^{(6)}, \quad B^* = \overline{\varphi}^{(2)} - \overline{\varphi}^{(1)}, \quad C^* = \overline{\varphi}^{(3)} - \overline{\varphi}^{(2)},$$
$$D^* = \overline{\varphi}^{(4)} - \overline{\varphi}^{(3)}, \quad E^* = \overline{\varphi}^{(5)} - \overline{\varphi}^{(4)}, \quad F^* = \overline{\varphi}^{(6)} - \overline{\varphi}^{(5)}.$$

Here $\hat{\Phi}_r$ is the piece-wise constant characteristic functions on the B-cell $\hat{\Omega}_R^h$.

3. The wind-stress forcing term is discretized on the B-cell.

$$\left(\mathrm{rot}_z\left(\frac{\tau}{\rho_0 H}\right), \hat{\Phi}_R\right)_{\hat{\Omega}_R^h} = \int_{\hat{\Gamma}_R}\left[\left(\frac{\tau_\lambda}{\rho_0 H}\right)\cos(l,\lambda) + \left(\frac{\tau_Q}{\rho_0 H}\right)\cos(l,\theta)\right]d\hat{\Gamma}_R,$$

where $\hat{\Gamma}_R$ is the contour of $\hat{\Omega}_R^h$, l is the tangent direction to $\hat{\Gamma}_R$.

Denoting by $\overline{\varphi}^{ab} = \varphi_a + \varphi_b/2$, and $|ab| = \mathrm{meas}(a,b)$ – the length of the segment (a,b) one can write:

$$\left(\mathrm{rot}_z\left(\frac{\tau}{\rho_0 H}\right), \hat{\Phi}\right)_{\hat{\Omega}_R^h} = \overline{\frac{\tau_\theta}{\rho_0 H}}^{de}|de| - \overline{\frac{\tau_\theta}{\rho_0 H}}^{ab}|ab| + \gamma\left[\left(\overline{\frac{\tau_\lambda}{\rho_0 H} - \frac{\tau_\theta}{\rho_0 H}}\right)^{fa}|fa| + \right.$$
$$\left.\left(\overline{\frac{\tau_\lambda}{\rho_0 H} + \frac{\tau_\theta}{\rho_0 H}}\right)^{ef}|ef| + \left(\overline{\frac{\tau_\theta}{\rho_0 H} - \frac{\tau_\lambda}{\rho_0 H}}\right)^{cd}|cd| - \left(\overline{\frac{\tau_\lambda}{\rho_0 H} + \frac{\tau_\theta}{\rho_0 H}}\right)^{bc}|bc|\right], \quad (16)$$

$\gamma = 0.3\sqrt{10}$.

4. The forcing term, describing the joint influence of the baroclinicity and bottom relief is approximated in much the same manner as the wind-stress term by substituting the vector $(1/\rho_0 H)\int_0^H \nabla p\, dz$ to (16) instead of vector $\tau/\rho H$.

4. Discretization of the baroclinic velocity equations

The integral relations for the problem (11) in accordance with the Galerkin procedure by multiplying these equations by vector-functions and integrating by parts. As a result the integral relation for the node r has the form

$$\left(\frac{\partial U'}{\partial t}, \vec{\Phi}_r\right) + (BU', \vec{\Phi}_r) + \left((f-\delta)\vec{k}\times U', \vec{\Phi}_r\right) + \int_{D_r^h} \nu \frac{\partial U'}{\partial z}\frac{\partial \vec{\Phi}_r}{\partial z}dD +$$
$$\int_{D_r^h} A_L\left(m^2\frac{\partial U'}{\partial \lambda}\frac{\partial \Phi_r}{\partial \lambda} + n^2\frac{\partial U'}{\partial \theta}\frac{\partial \Phi_r}{\partial \theta}\right)dD - \int_{D_r^h} A_L(n^2 - m^2\cos^2\theta)U'\vec{\Phi}_r dD -$$

$$\int_{D_r^h} 2A_L m^2 \cos\theta k \times \frac{\partial U'}{\partial \lambda}\vec{\Phi}_r dD = -\frac{1}{\rho_0}\Big(\nabla P - \frac{1}{H}\int_0^H \nabla P dz, \vec{\Phi}_r\Big) + \vec{F}, \qquad (17)$$

$$\vec{F} = \int_S A_L \vec{\Phi}_r \frac{\partial U'}{\partial n} ds + \int_\Omega \Big(\nu \frac{\partial U'}{\partial z}\vec{\Phi}_r\Big)\Big|_{z=0}^{z=H} d\Omega - (I, \vec{\Phi}_r).$$

Coordinate vector-function $\vec{\Phi}_r$ has the values $(0, \Phi_r)$, $(\Phi_r, 0)$, where Φ_r is the piece-wise linear function, which has the value one at the node r and zero at any other nodes. Let us note that the cells D_R^h and Ω_r^h are shifted by direction on the value $h_\lambda/2$ relatively D_R^h and Ω_R^h.

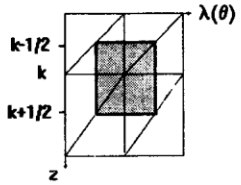

Figure 4. 3D C-cell; ZX(Y)-section

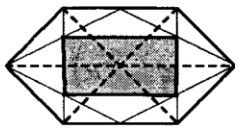

Figure 5. 3D C-cell; XY-section

1. Let us consider first the discretization of the advective terms represented by the integral form $(BU', \vec{\Phi}_r)_{D_r^n}$. Up-stream FEM analog is constructed with the lumping method on the circumcentric (C) - cell D_r^* (Figures 4, 5). For this purpose we denote piece-wise constant trial functions Φ_r, which is equal to one at the C-cell D_r^*. Advective terms can be written in the form:

$$BU' = m\Big[\Big(-\frac{\partial}{\partial\lambda}U'\frac{\partial\hat{U}}{\partial z} + \frac{\partial}{\partial z}U'\frac{\partial\hat{U}}{\partial\lambda}\Big) + \Big(-\frac{\partial}{\partial\theta}U'\frac{\partial}{\partial z}\frac{n}{m}\hat{U} + \frac{\partial}{\partial z}U'\frac{\partial}{\partial\theta}\frac{n}{m}\hat{U}\Big)\Big].$$

Then the integral relations for the advective terms can be written as follows:

$$(BU', \Phi_r^*) \approx I^\lambda(U, U^*) + I^\theta(U', U^*),$$

$$I^\lambda(U', U^*) = \int_{D_r^*} m\Big[\frac{\partial}{\partial\lambda}\Big(-U'\frac{\partial\hat{U}}{\partial z}\Big) + \frac{\partial}{\partial z}U'\frac{\partial\hat{U}}{\partial\lambda}\Big]\vec{\Phi}^* dD -$$
$$\int_{D_r^*} mU_r^*\Big[\frac{\partial}{\partial\lambda}\Big(-\frac{\partial\hat{U}}{\partial z}\Big) + \frac{\partial}{\partial z}\Big(\frac{\partial\hat{U}}{\partial\lambda}\Big)\Big]\vec{\Phi}_r^* dD,$$

$$I^\theta(U', U^*) = \int_{D_r^*}\Big[\frac{\partial}{\partial\theta}\Big(-U'\frac{\partial\hat{U}}{\partial z}\frac{n}{m}\Big) + \frac{\partial}{\partial z}U'\frac{\partial}{\partial\theta}\Big(\frac{n}{m}\hat{U}\Big)\Big]\vec{\Phi}_r^* dD -$$
$$\int_{D_r^*} mU_r^*\Big[\frac{\partial}{\partial\theta}\Big(-\frac{\partial}{\partial z}\frac{n}{m}\hat{U}\Big) + \frac{\partial}{\partial\theta}\Big(\frac{n}{m}\hat{U}\Big)\Big]\vec{\Phi}_r^* dD,$$

where U^* is the piece-wise constant function $U^* = \sum_{r\in D^h} U_r'\Phi_r^*$. From the latter relations with the use of the Green formula one can obtain

$$I^{\lambda}(U', U^*) = \frac{h_\theta}{n} \int_{\Gamma^*_{\lambda z}} (U^*_r - U') \frac{\partial \hat{U}}{\partial l} d\Gamma \equiv I^{\lambda}_r(U', U^*),$$

$$I^{\theta}(U', U^*) = \frac{h_\lambda}{m} \int_{\Gamma^*_{\theta z}} (U_r - U') \frac{\partial \hat{U}}{\partial l} d\Gamma \equiv I^{\theta}_r(U', U^*).$$

Here $\Gamma^*_{\lambda,z}$, $\Gamma^*_{\theta z}$ are the contours limiting the cell D^*_r at the cross-sections (λ, z), (θ, z) accordingly. Positive directions of the integrating is counter-clockwise.

Function U' according to the up-stream technique is calculated by the formula

$$U' = \sum_{A \in D^*_r} (U_A \vec{\lambda}_A - (1 - \vec{\lambda}_A) U_A), \quad \lambda_A = (\lambda^{\lambda}_A, \lambda^{\theta}_A),$$

where

$$\lambda^{\lambda}_A = \begin{cases} 1, & \text{if } \partial \hat{U}/\partial \lambda > 0, \\ 0, & \text{if } \partial \hat{U}/\partial \lambda \le 0, \end{cases} \qquad \lambda^{\theta}_A = \begin{cases} 1, & \text{if } \partial/\partial\theta(n/m\hat{U}) > 0, \\ 0, & \text{if } \partial/\partial\theta(n/m\hat{U}) \le 0. \end{cases}$$

Finally, the discrete form of the advective terms can be presented by the relations:

$$I^{\lambda}_r(U', U^*) = A_I U'_A + D_I U'_D + R^{\lambda}_1 U'_r(k-1) + R^{\lambda}_2 U'_r(k+1) + R^{\lambda}_I U'_r(k),$$

$$I^{\theta}_r(U', U^*) = B_I \frac{U'_B + U'_C}{2} + F_I \frac{U'_F + U'_E}{2} + R^{\theta}_1 U'_r(k-1) + R^{\theta}_2 U'_r(k+1) + R^{\theta}_I U'_r(k),$$

$$A_I = \frac{\delta'_\lambda \hat{u} - |\delta'_\lambda \hat{u}|}{2} \frac{h_\theta}{n}, \qquad D_I = \frac{\delta''_\lambda \hat{u} - |\delta''_\lambda \hat{u}|}{2} \frac{h_\theta}{n},$$

$$R^{\lambda}_1 = \frac{\delta'_z \hat{u} - |\delta'_z \hat{u}|}{2} \frac{h_\theta}{n}, \qquad R^{\lambda}_2 = \frac{\delta''_z \hat{u} - |\delta''_z u|}{2} \frac{h_\theta}{n},$$

$$R^{\lambda}_I = -(A_I + D_I + R^{\lambda}_1 + R^{\lambda}_2),$$

$$B_I = \frac{\delta'_\theta(n/m\hat{u}) - |\delta'_\theta(n/m\hat{u})|}{2} \frac{h_\lambda}{m}, \qquad F_I = \frac{\delta''_\theta(n/m\hat{u}) - |\delta''_\theta(n/m\hat{u})|}{2} \frac{h_\lambda}{m},$$

$$R^{\theta}_1 = \frac{\delta'_z(n/m\hat{u}) - |\delta'_z(n/m\hat{u})|}{2} \frac{h\lambda}{m}, \qquad R^{\theta}_2 = \frac{\delta''_z(n/m\hat{u}) - |\delta''_z(n/m\hat{u})|}{2} \frac{h_\lambda}{m},$$

$$R^{\theta}_I = -(B_I + F_I + R^{\theta}_1 + R^{\theta}_2);$$

$$\delta'_\lambda \hat{u} = (\hat{u}_{k+1/2} - \hat{u}_{k-1/2})_{i-1/2}, \qquad \delta''_\lambda \hat{u} = (\hat{u}_{k-1/2} - \hat{u}_{k+1/2})_{i+1/2}.$$

Here index k denotes the number of the vertical layer, where the central node is situated.

2. Both evolution and Coriolis terms are approximated on the base of the mass-lumping method at the C-cell:

$$\left(\frac{\partial U'}{\partial t}, \Phi_r\right)_{D_r^h} \approx \frac{\partial U'_r}{\partial t} \Delta Z_k \sum_{i(r)} \frac{S\Delta_i}{3};$$

$$((f-\delta)K \times U', \Phi_r)_{D_r^h} \approx ((f-\delta)K \times U')_r \Delta z_k \sum_{i(r)} \frac{S\Delta_i}{3}.$$

3. For the discretization of the vertical mixing term the lumping technique with respect to the horizontal coordinate is used. That means that the coordinate functions in this case are piece-wise linear by the vertical and piece-wise constant by the horizontal coordinates. So, the discrete form is as follows:

$$\int_{D_r^h} \nu \frac{\partial U'}{\partial z} \frac{\partial \Phi_r}{\partial z} dD = \sum_{i(r)} \int_{\Delta i^z} \nu \frac{\partial U'}{\partial z} \frac{\partial \Phi_r}{\partial z} dD = \sum_{i(r)} \int_{\Delta_i} \int_{Z_{k-1}}^{Z_{k+1}} \nu \frac{\partial U'}{\partial z} \frac{\partial \Phi_r}{\partial z} dS$$

$$= \left[\frac{\nu_{k-1/2}}{\Delta Z_{k-1/2}}(U'_k - U'_{k-1}) - \frac{\nu_{k+1/2}}{\Delta Z_{k+1/2}}(U'_{k+1} - U'_k)\right] \sum_{i(r)} S\Delta_i,$$

$$k = \overline{1, N_z}, \quad \nu_{1/2} = \nu_{N_{z+1/2}} = 0.$$

4. To obtain the discrete operator for the term, describing horizontal diffusion the interpolating functions are chosen piece-wise constant by the vertical and piece-wise linear by the horizontal coordinates

$$\int_{D_r^h} A_L \left(m^2 \frac{\partial U'}{\partial \lambda} \frac{\partial \Phi_r}{\partial \lambda} + n^2 \frac{\partial U'}{\partial \theta} \frac{\partial \Phi_r}{\partial \theta}\right) dD =$$

$$\sum_{i(r)} \Delta Z_k \int_{\Delta_i} A_L \left(m^2 \frac{\partial U'}{\partial \lambda} \frac{\partial \Phi_r}{\partial \lambda} + n^2 \frac{\partial U'}{\partial \theta} \frac{\partial \Phi_r}{\partial \theta}\right) d\Omega,$$

$$\int_{\Delta_i} A_l \left(m^2 \frac{\partial U'}{\partial \lambda} \frac{\partial \Phi_r}{\partial \lambda} + n^2 \frac{\partial U'}{\partial \theta} \frac{\partial \Phi_r}{\partial \theta}\right) d\Omega =$$

$$S_{\Delta_i} A_L \left[\overline{m^2}^{\Delta_i} \left(\frac{\partial}{\partial \lambda} \sum_{j=1}^{3} U'_j \Phi_j\right) \frac{\partial \Phi_r}{\partial \lambda} + n^2 \left(\frac{\partial}{\partial \theta} \sum_{j=1}^{3} U'_j \Phi_j\right) \frac{\partial \Phi_r}{\partial \theta}\right],$$

where j has the values of the vortices of i-th triangle. As the result the discrete operator for the diffusion term can be written as follows:

$$\int_{D_r^h} A_L \left(m^2 \frac{\partial U'}{\partial \lambda} \frac{\partial \Phi_r}{\partial \lambda} + n^2 \frac{\partial U'}{\partial \theta} \frac{\partial \Phi_r}{\partial \theta}\right) dD =$$

$$A_L \sum_{i(r)} S\Delta_i \sum_j U'_j \left[\overline{m^2}^{\Delta_i} \frac{\partial \Phi_j}{\partial \lambda} \frac{\partial \Phi_j}{\partial \lambda} + n^2 \frac{\partial \Phi_j}{\partial \theta} \frac{\partial \Phi_r}{\partial \theta}\right],$$

$$\int_{D_r^h} A_L(n^2 - m^2\cos^2\theta)U'\Phi_r dD =$$

$$A_L(n^2 - m^2\cos^2\theta)_r U'_r \Delta Z_{k-1/2} \sum_{i(r)} \frac{S\Delta_i}{3},$$

$$\int_{D_r^h} A_L m^2 \cos\theta \frac{\partial U'}{\partial\lambda}\Phi_r dD =$$

$$A_L \Delta Z_{k-1/2} \sum_{i(r)} \overline{m^2\cos\theta}^{\Delta_i} \frac{S\Delta_i}{3} \sum_{j(i)} \left(U' \frac{\partial\Phi_j}{\partial\lambda}\right),$$

$$k = \overline{1, Nz}, \quad \Delta Z_{1/2} = 0.$$

5. Finally, let us come to the pressure gradient approximation. First of all we remind that the nodes with which the pressure is associated are shifted on the half of the step h relatively the velocity nodes. In this case the pressure gradient operator will have a form of centered derivatives relatively node r. Denoting the pressure nodes, surrounding the velocity node r by R, C, D, E, the operator can be written in the form

$$\left(m\frac{\partial P}{\partial\lambda}, \Phi_r^*\right) \approx \overline{\vec{m}^r} S_r \frac{P_D - P_r}{h\lambda}, \qquad \left(n\frac{\partial P}{\partial\theta}, \Phi_r^*\right) \approx \bar{n}^r \frac{P_c - P_r}{2he},$$

where S_r is the measure of the support of the quadrangle $RCDE$ and the overbar denotes the averaging over this support.

5. Realization with respect to time

Equations can be rewritten in the operator form

$$\frac{\partial U'_r}{\partial t} + \Lambda_\zeta U'_r + \Lambda_k U'_r + \Lambda_\nu U'_r + \Lambda_L U'_r = F_r, \tag{18}$$

where:

Λ_ζ – the advective operator,

Λ_k – the Coriolis term,

Λ_ν – the vertical diffusion operator,

Λ_L – the horizontal diffusion operator,

F_r – the right-hand side of the equation.

The horizontal diffusion term is calculated by the explicit procedure at the time level $(p-1)$ and the vertical diffusion term by implicit one at the level (p). For the Coriolis term, the semi-implicit presentation is used [8]

$$\Lambda_k U_r' = \Lambda_k [U_r'^{(p-1)} + \alpha (U_r'^{(p)} - U_r'^{(p-1)}], \alpha \epsilon [0, 1].$$

After linearization relatively time level (p) advective operator is partitioned into two parts, $\Lambda_\zeta = \Lambda_\zeta^w + \Lambda_\zeta^u$, where Λ_ζ^w is the operator acting along the vertical direction and Λ_ζ^u – along the horizontal directions. The first part is attributed to the implicit time step, whereas the latter one is calculated at the explicit time step. As a result (18) can be written in the form

$$\frac{\partial U_r'}{\partial t} + [\Lambda_\zeta^w + \alpha \Lambda_k + \Lambda_\nu] U_r'^{(p)} = P_r - [\Lambda_L + \Lambda_\zeta^u + (1 - \alpha) \Lambda_k] U_r'^{(p-1)}. \quad (19)$$

The system of equations (19) is resolved by the matrix factorization method.

6. Results of diagnostic calculations

6.1. Monthly averaged climatic integral stream function

Quasi-stationary solutions of (12) were obtained. Monthly averaged wind-stress [2] is used as forcing. The solution for $R = 0.5$ cm/s is presented in [9]. One can see that in the northern part of the basin the highest intensity of the gyres is reached during the winter season and the lowest – in summer. In the southern part, the distribution is opposite. This fact has been marked in the works [2, 4, 5].

The reason of this behavior of the solution is the deeper extrema of the wind-stress rotor in the northern hemisphere in winter. The centers of the gyres of the integral stream function (ISF) correspond to the local extrema of $\mathrm{rot}_z \tau$ with the cyclonic circulation in the zones with minima of ISF and anticyclonic rotation corresponding to the zones with the maximum. Absolute values of the $\mathrm{rot}_z \tau$ define the intensity of the gyres. The results of the calculation show that in the Kuroshio region south of Japan the highest values of the mass transport are reached in the winter time (appr. 30 Sv.), which is correlated with the wind-stress rotor. However this result is notin agreement with the observations of the Kuroshio mass transport being calculated by the sea level differences [4]. This fact indicates that the reason of the annual variations of the Kuroshio mass transport is not connected directly with the wind-stress distribution. On the other hand, the inclusion of the integral influence of baroclinicity to the right- hand side of the vorticity equation as an additional forcing term leads to the results with the mass transport maximum in summer [9].

The decrease of the bottom friction causes some intensification of the barotropic currents. The quantitative variations of the mass transport are presented in the table with the comparison with the results [2], obtained by Sverdrup's relations.

Integral mass transport by the western boundary currents

Month	latitude	[2]	$R = 5 \cdot 10^{-1}$ cm/sek	$R = 5 \cdot 10^{-2}$ cm/sek
January	48° N	50 ± 40	20	30
July	52° N	10	5	8
January	30° N	90 ± 12	59	80
July	30° N	40	38	47
January	6° N	50 ± 14	27	40
July	11° N	30	8	18

Let us consider now the anomalies of the monthly averaged values of ISF from the seasonal values, presented in Figure 6. The results are obtained in the following way: seasonal values of the ISF are denoted by the averaging over three months. The months for the seasons are as follows: Winter (February–April), Spring (May–July), Summer (August–October), Fall (November–January).

For the analysis of the results three zones are separated: A (30° N – 60° N), B (10° N – 30° N), C (10° S – 10° N). Then, the seasonal values of the ISF were subtructed from the monthly values and the extrema of these deviations were evaluated for each zone. The graphs presented in Figure 6 are drawn by these values. Let us consider the results for each zone.

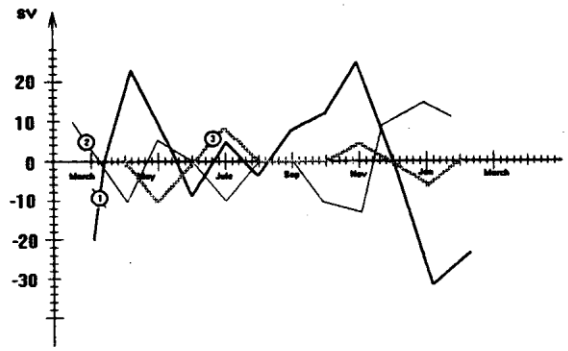

Figure 6. The extrema value of anomalies (Sv) (monthly-seasonal): 1 – A-zone; 2 – B-zone; 3– C-zone

Zone A (Subpolar frontal zone). The most essential variations of the amplitude are observed in the winter months. In the spring time, the variations decrease, and in summer they are small. The reason of nonstable circulation in winter is connected with the transformation of the wind-stress field which has the high activity in this zone of subpolar front and is causes by the interaction between the Siberian High and the Aleutian Low which is very intensive in this period.

Zone B (Subtropical frontal zone). The transformation of the mass transport during the seasons still exists, but is significantly weaker than in A-zone. The fall-winter months also have the highest activity but the maximal values of the anomalies reach only 25 Sv. against 60 Sv. for the same period in Zone A.

Zone C (Equatorial frontal zone). This zone is characterized by the minimal values of the variations both in the summer and in the winter seasons. ISF distribution is characterized by the dipole structure, the cyclonic gyre – to the North of the equator and anticyclonic one – to the south. In spring the anticyclonic circulation increases whereas cyclonic one decreases and in fall – vise versa. In Figure 7 deviations in the A- and C-zones are positively correlated and are in the antiphase with the deviations in B-zone.

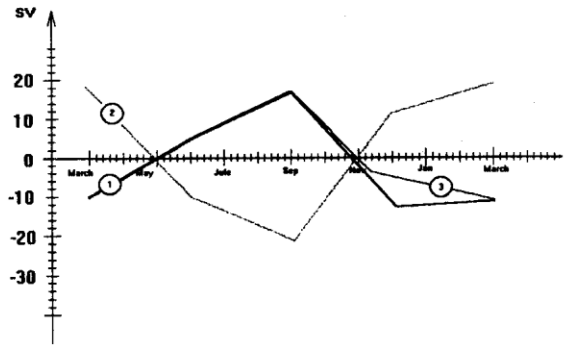

Figure 7. The extrema value of anomalies (Sv) (seasonal-annual): 1 – A-zone; 2 – B-zone; 3 – C-zone

6.2. Diagnostic calculations of the 3D velocity field

Diagnostic calculations for the winter season on the basis of the temperature and the salinity Levitus data were carried out. The calculations began with the state of rest. In the first 5 days an abrupt increase of the kinetic energy was observed. After this period the increase became weaker reaching 1 per cent by the 7-th day. By that time all main components of the circulation system were formed (Figures 8, 9). The mass transport in the Kuroshio current attends the value of 45 sv. The results show two trajectories of the current south of Japan. One of them passes along the shore of Japan and the other branch goes round the Idzu ridge from the south.

The values of the velocity in the Kuroshio jet are about 45 cm/s. At the depth 600 m the Kuroshio current changes direction and at the lower layers countercurrent exists. In the equatorial zone the behavior of the velocity field is very disordered, which is typical of diagnostic calculations.

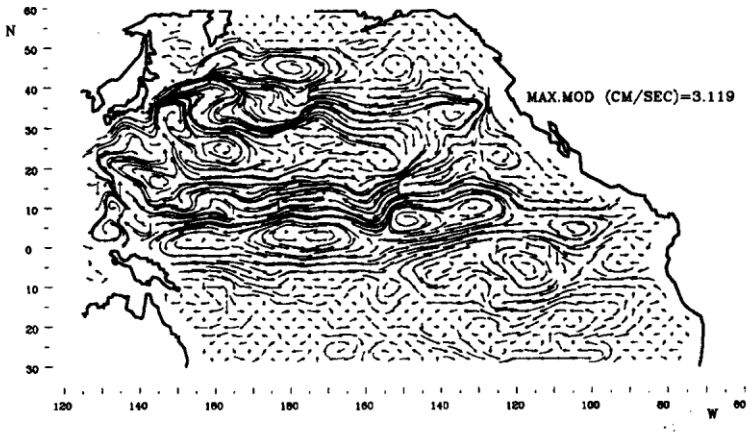

Figure 8. Diagnose. Barotropic velocity

In the upper 200 m, the analysis of the vertical velocity sign (Figure 10) shows regular zones of the upwelling and downwelling connected with the cyclonic and anticyclonic circulation of the main gyres. In the layer lower than 600 m the picture of the vertical velocity component sign is not so regular. This is connected with increasing the influence of the baroclinicity and bottom relief, which began to play more important role in the lower layers than the wind-stress forcing. This strong influence of the bottom relief is also the reflection of the unbalanced temperature/salinity fields and bottom relief.

Meridional heat flux (Figure 11), obtained by the diagnostic results gives more or less correct direction to the north of the equator (to the North Pole), but in the equatorial zone the unreally strong Ekman cell leads to the unrealistic peaks in the heat flux. This fact also confirms the fact that the diagnostic procedure is ill-posed in the mathematical and physical sense, and the situation may improves with the integration of the whole system of equations.

7. Conclusion

1. Barotropic circulation has mainly an adequate distribution by zones, but when the forcing is determined only by the wind-stress, then the annual cycle of the subtropical gyre is in antiphase with the observations. Including the integral influence of the baroclinicity to the forcing term gives more realistic distributions mass transport with respect to time. This indicates that the annual variations of the baroclinic structure are more essential for the annual mass transport than the direct wind forcing.

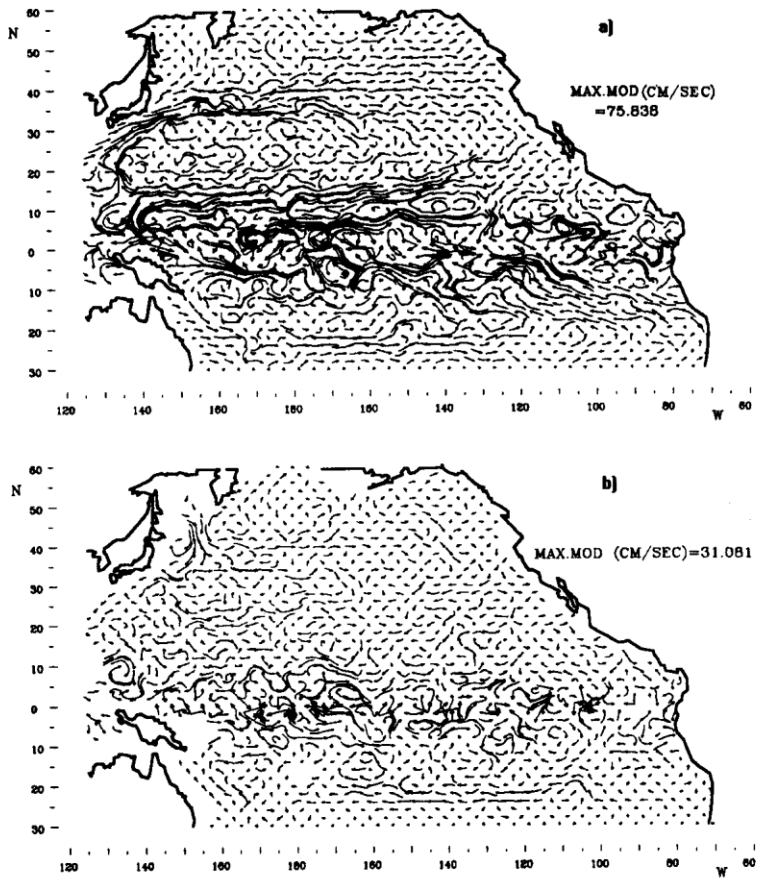

Figure 9. Diagnose. Velocity field on: a) 50 m, b) 600 m

2. Analysis of the interseasonal variability of the integral stream function shows that in the North Pacific there are both zones with a more stable circulation structure and zones with the intensive inter seasonal variability of the mass transport. The maximal variability of the subpolar and subtropical frontal zones are reached in the fall-winter months. The phases of the interseasonal variability are positively correlated in the subpolar and equatorial frontal zones and they both are negatively correlated with the variations with the subtropical frontal zone.

3. In the 3D diagnostic calculations the unbalance between the temperature, salinity fields and the bottom relief leads to some inconsistency of the results, espesially in the equatoral zone. The fields may be reduced to the balance by the whole system time integration, for a certain period. After this period the geostrophical adjustment processes may lead the system to the balance.

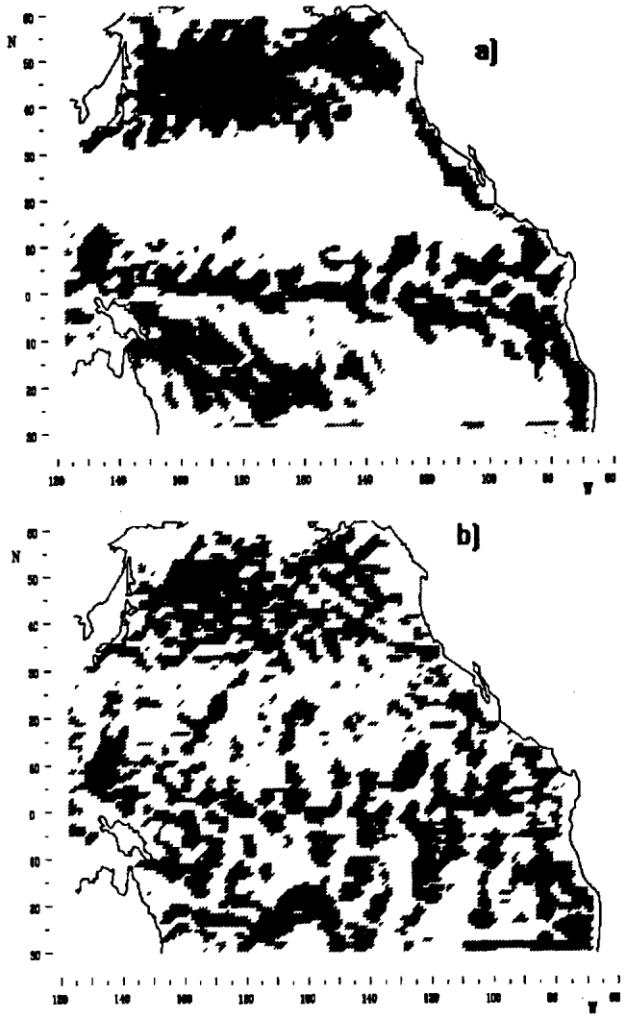

Figure 10. Sign of the vertycal velocity: a) z=50 m, b) z=600 m

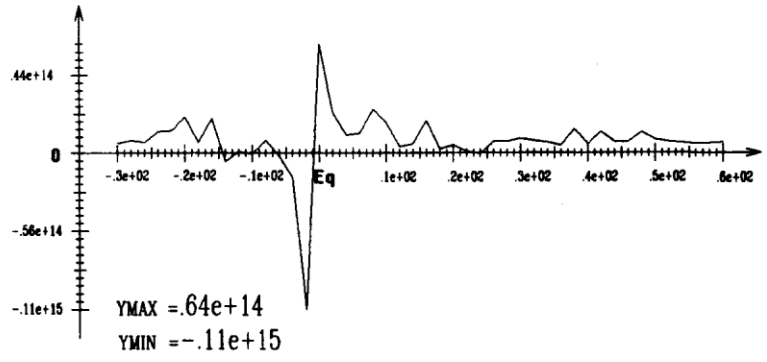

Figure 11. Meridional heat flux

References

[1] V.I. Kuzin, *The Finite Element Method in the Ocean Processes Modelling*, Novosibirsk, Computing Center, 1985, 190 p. (in Russian).

[2] S. Hellerman, M. Rosenstein, *Normal monthly wind-stress over the World Ocean with error estimates*, J. Phys. Oceanogr., Vol. 13, No. 7, 1983, 1093–1104.

[3] S. Levitus, *Climatological Atlas of the World Ocean*, Environmental Res. Lab., Geophys. Fluid Dynamics Lab., Princeton, N.J. Rockville, Md December, 1982.

[4] R.G. Greatbuch, S.A. Gouling, *Seasonal variations in a linear barotropic model of the North Pacific driven by the Hellerman and Rosenstein Wind stress field*, J. Geophys. Res., Vol. 94, C9, 1989, 12645–12665.

[5] J. Cherniavsky, G. Holloway, *Sensitivity of the upper ocean GCM to wind stress climatology*, Res. Activities in Atmospheric and Oceanic Modelling Rep. 17, 1992, 8.32–8.34.

[6] G.I. Marchuk, *Numerical Solution of the Problems of the Atmosphere and Ocean Dynamics*, Leningrad, Gidrometeoizdat, 1972 (in Russian).

[7] A. Arakawa, *Design of the VGLA general circulation model*, Dep of Meteorology, Univ. of California, Los Angeles, Numerical Simulation of Wearther and Climate, Tech. Rept., No 7, 1972.

[8] A.Y. Semtner, *An oceanic general circulation model with bottom topography*, Univ. of California, Los Angeles, Numerical simulations of Wearther and Climate, Tech. Rept., No. 7, 1974.

[9] V.I. Kuzin, V.M. Moiseev, *Model of the North Pacific circulation*, Proc. of Computing Center SD RAS, Issue 1, 1993, 19–46 (in Russian).